Magma Mixing Models for Merensky-Style Mineralization - The Fallacy of Binary Diagrams

R. Grant Cawthorn

Department of Geology, University of the Witwatersrand, PO Wits, 2050, South Africa
e-mail: 065rgc@cosmos.wits.ac.za

Summary

Magma mixing has been proposed as a mechanism for the production of immiscible sulfide liquids, using binary diagrams to define sulfur-saturation limits. The same curve has been used for fractionating magmas and for their products of mixing between end-members. This assumption is invalid because the two magma series have different compositions, especially with respect to iron contents. A reassessment of magma mixing shows that mixed magmas of Bushveld affinity do not reach sulfur saturation.

With respect to the Merensky Reef and UG2 chromitite, the immediate hangingwalls appear to be sulfur-undersaturated, based on analyses for S and Cu. The concept that the fractionating magma may go through a phase of sulfur undersaturation is not supported by a detailed examination of the geometry of the phase diagram.

The mechanism for sulfide-associated, platinum-group element mineralization needs to be re-examined.

Sulfur-Saturation Diagrams

There are differences between magma series produced by fractionation and those produced by magma mixing, and these differences need to be clearly recognized. In the present case, the original calculations of Naldrett and von Gruenewaldt (1989) were presented relating the solubility of sulfide to the percent of fractionation of the Bushveld parental magma. The selection of the abscissa as the weight percent crystallized makes it impossible to infer the chemical composition of such magmas. This axis is not a linear chemical parameter. Hence it cannot be assumed that mixing of two magmas will follow a straight line on the diagram or that percentages of mixing will necessarily be equally spaced between the two compositions being mixed (Cawthorn, 1999). Recognizing this limitation, Li et al. (2001) modified the original diagram and plotted Zr as the abscissa (Fig. 1). They also recalculated the sulfur solubility limits for the evolving magmas based on the empirical equation:

$$S = 1431 + 221 \times (FeO - 9) + 5 \times (T-1200) \quad (1)$$

where S is sulfur solubility in ppm, FeO is molar percent, and T is temperature in ^{o}C. This equation emphasizes the major role of iron and temperature in controlling sulfur solubility as originally shown by Haughton et al. (1974).

The revised diagram of Li et al. (2001) shown in Fig. 1c, has a different topology from that presented by Naldrett and von Gruenewaldt (1989), in that once plagioclase and orthopyroxene begin to coprecipitate the solubility of sulfur in residual magmas increases. This effect is the consequence of decreasing iron content during mafic mineral crystallization, followed by increasing iron content during norite fractionation. The consequences of magma mixing with regard to this diagram require careful re-examination. Li et al. (2001) assumed addition of primitive magma of composition A in Fig. 1. Mixing with residual magma (point R in Fig. 1) produced compositions lying along the line AR.

The compositions of fractionating and mixed magmas are different. The composition, C, generated during the fractionation process at the temperature where plagioclase begins to crystallize, and containing 112 ppm Zr is shown in Fig. 1 and Table 1. A magma produced by mixing of one part A (with 80 ppm Zr) and three parts R (with 123 ppm Zr) yields 112 ppm Zr, the same for composition C. Similar calculations for all elements give composition M in Fig. 1. Compositions M and C are distinctly different especially in terms of FeO (Fig. 1b). The important conclusion is that the compositions of the series of magmas defined by fractionation (e.g. C) are not the same as those produced by mixing of two end-members (e.g. M) from that fractionation series.

The difference between fractionation and mixing can be visualized by reference to Fig. 2, a phase diagram showing the relationships in the system plagioclase - orthopyroxene - clinopyroxene. The designated points in this diagram are the same as those shown in Fig. 1. Fractionation of composition A produces a trend through C to R, whereas mixing between A and R produces a trend through M. It should be noted, for example, that the mixing curve from R to A produces compositions all of which lie in the orthopyroxene field. However, in Fig. 1c, the

implication is that mixing of A into R produces liquids that are still saturated with both plagioclase and orthopyroxene until point M is passed, which is not correct. The important inference is that compositions C and M are chemically different and it should not be assumed that they would have the same sulfur saturation limits.

The essence of the model proposed by Li et al. (2001) is that they assume that because compositions C and M have the same Zr content they will have the same sulfur saturation limits. In Fig. 1a it can be seen that the mixing of compositions A and R produces a series of liquids that have higher temperatures than those produced during fractionation of composition A (curves RMA versus ABCR in Fig. 1a). Second, the mixing curve RMA yields mixed magmas with higher FeO contents than fractionated magmas along curve ABCR (Fig. 1b). The combined effect of higher temperature and higher FeO contents during mixing (point M) results in higher sulfur solubilities than for fractionation (point C), when the above equation 1 is used. The sulfur solubilities for magmas produced during mixing define a straight line from R to P (the latter being the sulfur solubility of magma A) that exceed the solubilities of the iron-depleted fractionation trend PCR (Fig. 1c). As a result point M lies below the sulfur saturation curve for mixed magmas. The same criticism applies to the original diagram of Naldrett and von Gruenewaldt (1989), since they also assume that fractionation and mixing produce identical magmas with identical sulfur solubility limits.
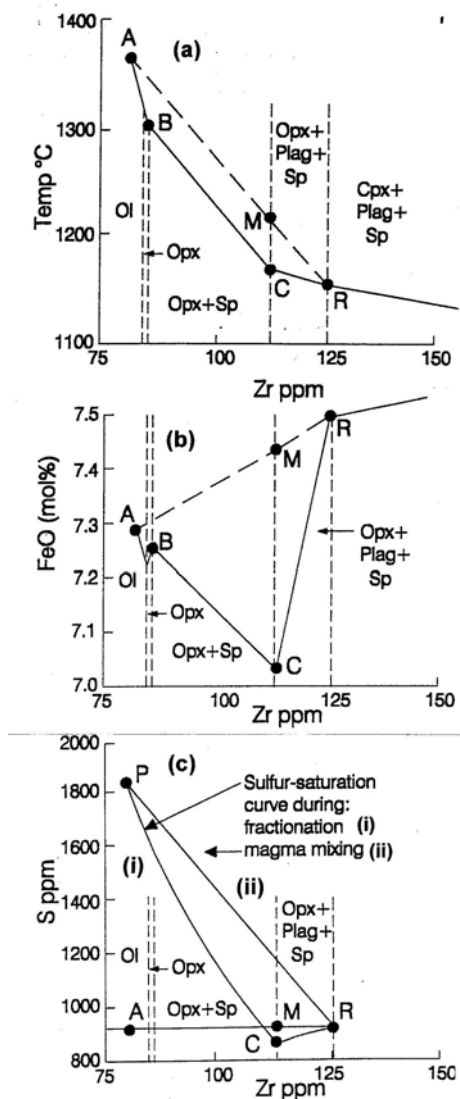
Figure 1. Sulfur solubility as a function of various parameters related to the evolution of the parental magma to the Bushveld Complex. Zr is used as the abscissa in all plots as suggested by Li et al. (2001). In all diagrams A is the parental magma to the Bushveld Complex and claimed by Naldrett and von Gruenewaldt (1989) and Li et al. (2001) to be the magma added at the Merensky Reef; B is the composition at orthopyroxene and spinel saturation; C is the composition at which plagioclase begins to crystallize; R is the residual magma present in the chamber immediately prior to the formation of the Merensky Reef, M is a mixed magma (A:R in the ratio 1:3) calculated to have the same Zr content as C. Analyses A, B, C and R are taken from Li et al. (2001). The silicate mineral stability fields and temperature are also taken from Li et al. (2001). (a) Plot of temperature versus Zr showing that the mixing trend RA produces magmas of higher temperature than the fractionation trend ABCR. (b) Plot of FeO (in mole %) versus Zr. The fractionation trend can be seen to display a marked minimum in iron content at the onset of plagioclase fractionation, whereas the mixed magmas do not display an iron minimum. (c) Plot of sulfur solubility, based on equation 1 and analyses in Table 1, versus Zr. The curve, PCR, determined by Li et al. (2001) from the compositions of fractionating magmas, is shown. Using the FeO contents and temperatures presented in the upper two diagrams and equation 1 in the text, the sulfur solubility for mixed magmas is shown as the straight line, PR. Note that mixed magma, M, lies above the sulfur solubility curve for fractionating magmas, but below the solubility curve for mixed magmas.

Figure 2. *Phase relations in the system orthopyroxene - clinopyroxene - plagioclase. The points A, C, R and M are the same as used in Fig. 1. Note that the compositions of a mixed magma, M, and that of the fractionated magma, C, are very different. The olivine stability field is ignored for simplicity.*

Figure 3. *Plot of S versus Zr. The data used to construct curve SCRE are taken from the appendix 2 and Fig. 4 of Li et al. (2001). This diagram is extended to the origin (0 ppm S, 0 ppm Zr) to show the composition of cumulates. Trends AS and CF result from fractionation of cumulates with zero S and Zr. Trend CR results from the removal of cumulates of composition D.*

The geological consequences of Fig. 1c are that the product of mixing of residual magma R with added magma A is a mixed magma that has a different composition from that produced during fractionation. The mixed magmas (RMA) have greater sulfur solubility than the fractionated magmas (ABCR), and as a consequence the mixed magmas are not sulfur saturated. The problem lies in the assumption that a phase boundary on a binary diagram can be used for any natural magma composition. It can not. It can only be applied to the specific magma compositions for which it was calculated. The criticism here of assuming that the phase field is uniquely defined in a binary diagram for natural magmas is not confined to that of sulfur

solubility, but applies to all such diagrams whatever the axes and whatever mineral is being considered.

Sulfur Undersaturation

The layered cumulates immediately above the Merensky and UG2 chromitite reefs do not appear to be sulfide bearing (Cawthorn, 1999). Such a situation is not consistent with the hypothesis of magma mixing. To produce sulfide saturation that model requires a large volume of mixed magma of composition C (Fig. 1) to have formed. Further fractionation of this magma ought to have produced cumulate rocks containing immiscible sulfide, as the liquid evolves along CR. It has been suggested that along this curve sulfur undersaturation is achieved (Li et al., 2001), but this interpretation is questioned here. The relationships are shown in Fig. 3. The parental magma, A, initially fractionates a sulfide-free assemblage that will plot at the origin in the S versus Zr diagram. Once the magma reaches point S it will become sulfide-saturated and an immiscible sulphide liquid forms and the liquid evolves along curve SC. Because the FeO content of the remaining magma also drops (see Fig. 1b), so does the S solubility. The increase in sulfur solubility from C to R relates to the increase in FeO in the remaining magma during norite fractionation. However, inspection of Fig. 3 shows that fractionation must remain sulfur-saturated. The trend for fractionation of a sulfide-free assemblage from composition C would lie along CF, being a projection from the origin (0 ppm Zr and 0 ppm S) representing the composition of the crystallizing assemblage, through point C. Since the increase in sulfur in trend CF exceeds that in CR the process of sulfur-undersaturated fractionation is impossible. The difference between trend CR and CF is very small, and so it necessary to confirm such differences by reference to the exact compositions involved. Composition C contains 112 and 824 ppm of Zr and S respectively, and for R the values are 123 and 885 ppm respectively (Li et al., 2001). The increase in Zr is therefore by a factor of 1.098, whereas for S it is only 1.074. The difference between these two values is small, but the smaller increase in S compared to Zr means that S must have been more compatible than Zr, and that some sulfide fractionation is required. In fact, to produce the average trend form C to R requires the removal of a bulk cumulate of composition D (CD being the back projection of CR) in Fig. 3 that has 200 ppm S and 0 ppm Zr. Thus, the cumulates formed during norite fractionation must contain a small proportion of sulfide (approximately 0.05%), in contradiction of the suggestion by Li et al. (2001), and the observations made on the rocks (Cawthorn, 1999).

References

Cawthorn, R.G., 1999, Platinum-group element mineralization in the Bushveld Complex - a critical reassessment of geological models: South African Journal of Geology, v. 102, p. 268-281.

Haughton, D.R., Roeder, P.L., and Skinner, B.J., 1974, The solubility of sulfur in mafic magmas. Economic Geology, v. 69, p. 451-462.

Li, C., Maier, W.D., and de Waal, S.A., 2001, The role of magma mixing in the genesis of PGE mineralization in the Bushveld Complex: thermodynamic calculations and new interpretations: Economic Geology, v. 96, p. 653-662.

Naldrett, A.J., and von Gruenewaldt, G., 1989, Association of platinum-group elements with chromitite in layered intrusions and ophiolite complexes: Economic Geology, v. 84, p. 180-187.